NUCLEON SHADOWING IN GLAUBER MODELS*

Sandeep Chatterjee†, Snigdha Ghosh, Sushant K. Singh
Md. Hasanujjaman, Jane Alam, Sourav Sarkar

Theoretical Physics Division, Variable Energy Cyclotron Centre
1/AF Bidhannagar, Kolkata, 700064, India

(Received June 14, 2016)

The two-component Monte Carlo Glauber model predicts a knee-like structure in the centrality dependence of elliptic flow v_2 in U+U collisions at $\sqrt{s_{NN}} = 193$ GeV. It also produces a strong anti-correlation between v_2 and $\mathrm{d}N_{\mathrm{ch}}/\mathrm{d}y$ in the case of top Zero Degree Calorimeter (ZDC) events. However, none of these features have been observed in data. We address these discrepancies by including the effect of nucleon shadowing to the two-component Monte Carlo Glauber model. Apart from addressing successfully the above issues, we find that the nucleon shadow suppresses the event-by-event fluctuation of various quantities, *e.g.* ε_2 which is in accordance with expectation from the dynamical models of initial condition based on gluon saturation physics and is in very good agreement with experimental data at $\sqrt{s_{NN}} = 2760$ GeV for Pb+Pb collisions.

DOI:10.5506/APhysPolBSupp.9.197

1. Introduction

One of the most important ingredients in understanding the evolution of matter formed in heavy-ion collisions (HIC) is its initial condition (IC). Currently, there are several models of IC available with varying degrees of success in explaining the data [1–12]. The Monte Carlo-based IC models generate the event-by-event (E/E) fluctuations in observables which can be compared to those measured in experiments. Most of these models share the first step — sampling the positions of the constituent nucleons of the two colliding nuclei from their nuclear density distribution which is usually taken to be a Woods–Saxon profile [13]. In the second step, they all differ in the energy deposition scheme corresponding to a specific configuration of the nucleon positions. This finally results in different predictions of centrality

* Presented by S. Chatterjee at WPCF 2015: XI Workshop on Particle Correlations and Femtoscopy, Warszawa, Poland, November 3–7, 2015.

† Corresponding author: mail2sandchatt@gmail.com

dependence of multiplicity, eccentricities and their event-by-event distributions. The largest source of uncertainties on the extracted values of the medium properties obtained by comparing the predictions of the theoretical models to data is known to stem from the choice of the IC [14].

Monte Carlo Glauber models (MCGMs) have been reasonably successful in describing the qualitative features of various observables [6,7]. The energy deposition scheme is largely geometrical with the only dynamical input being a constant nucleon–nucleon cross-section σ_{NN}. The recent data on $v_2 - \frac{\mathrm{d}N_{\mathrm{ch}}}{\mathrm{d}\eta}$ correlation for the top Zero Degree Calorimeter (ZDC) events in U+U collisions at $\sqrt{s_{NN}} = 193$ GeV and Au+Au interactions at $\sqrt{s_{NN}} = 200$ GeV [15] could not be reproduced within the ambit of the standard MCGM [11]. The MCGM predictions are also in disagreement with the E/E distribution of the second flow harmonic for Pb+Pb collisions at $\sqrt{s_{NN}} = 2.76$ TeV. However, dynamical models based on gluon saturation physics such as IP-Glasma [9] and EKRT [12] are in agreement with data.

MCGMs provide a simple and intuitive description of the IC and, hence, there have been considerable efforts to address the above issues within the geometric approach of the MCGM [10,16]. Recently, we have shown that the inclusion of shadowing effect due to the leading nucleons on those located deep inside provides a simple and physical picture that brings the predictions of the shadowed MCGM (shMCGM) in agreement with that of data [15,17,18] as well as dynamical models like IP-Glasma [9] at the top RHIC energy for Au+Au as well as U+U collisions [20] and for Pb+Pb collisions at $\sqrt{s_{NN}} = 2.76$ TeV [21]. The idea of nucleon shadowing inside a nucleus was first proposed long ago [19]. However, the phenomenological consequences in heavy-ion collisions have been rarely explored.

2. The model

The details of the shMCGM are given in Ref. [20,21]. Here, we summarise its main features. The shMCGM is an extension of the two-component MCGM. In the latter, the energy deposited at (x, y) on the plane transverse to the beam axis (which is along the z axis) is assumed to be a linear superposition of two terms — $N_{\mathrm{part}}(x, y)$ and $N_{\mathrm{coll}}(x, y)$, where N_{part} counts the number of participant nucleons and N_{coll} is the number of possible binary collisions between them. The total charged multiplicity $\mathrm{d}N_{\mathrm{ch}}/\mathrm{d}\eta$ is also assumed to have a similar linear relation with the total N_{part} and N_{coll}

$$\epsilon(x, y) = \epsilon_0 \left[(1-f) N_{\mathrm{part}}(x, y) + f N_{\mathrm{coll}}(x, y)\right] , \tag{1}$$

$$\frac{\mathrm{d}N_{\mathrm{ch}}}{\mathrm{d}\eta} = n_0 \left[\left(\frac{1-f}{2}\right) N_{\mathrm{part}} + f N_{\mathrm{coll}}\right] , \tag{2}$$

where ϵ_0 and n_0 are the overall normalization parameters for the energy deposited and multiplicity produced. f is usually called the hardness factor which is fixed by comparing with data. In the standard two-component MCGM approach, all the participants are treated democratically irrespective of their z coordinate. In the shMCGM, we introduce the effect of shadowing due to leading participants on the others through the following Ansatz

$$S(n,\lambda) = e^{-n\lambda}\,, \tag{3}$$

where $S(n,\lambda)$ is the shadowing effect on a participant due to n other nucleons from the same nucleus which are in front and shadow it. Thus, all the participants are no more treated on equal footing — the leading nucleons contribute to energy deposition more than those located deep inside. Thus overall, we have the following three parameters in the shMCGM — n_0, f and λ (see Table I) which are constrained by data on multiplicity and v_2 [20, 21].

TABLE I

The values of the parameters of the Glauber model used in this work [20, 21].

Model	$\sqrt{s_{NN}}$ [GeV]	System	n_0	f	λ
MCGM	200	Au+Au	2.37	0.14	—
MCGM	193	U+U	2.30	0.14	—
MCGM	2760	Pb+Pb	4.05	0.11	—
shMCGM	200	Au+Au	2.83	0.32	0.12
shMCGM	193	U+U	2.83	0.32	0.12
shMCGM	2760	Pb+Pb	4.05	0.32	0.08

3. Results

The ε_2 calculated within the ambit of MCGM and shMCGM have been used to obtain v_2 through the scaling $v_2 = \kappa\varepsilon_2$ with $\kappa \sim 0.2$ [22]. In Fig. 1 (left), we have compared the centrality dependence of this scaled ε_2 with the STAR data on $v_2\{2\}$ in U+U collisions [15]. We find a fairly good qualitative agreement between data and shMCGM. The most striking difference between shMCGM and MCGM occurs for the most central events where the effect of shadow is expected to be the highest. Clearly, the knee-like structure that is predicted by the MCGM (but not observed in data) is washed away in the case of shMCGM which accurately follows the data. The knee-like structure has vanished because the effect of shadowing moderates the collision process to bring a balance in the effective numbers of collisions for tip–tip and body–body geometry by reducing $N_{\rm coll}$ more in TT compared to BB configurations.

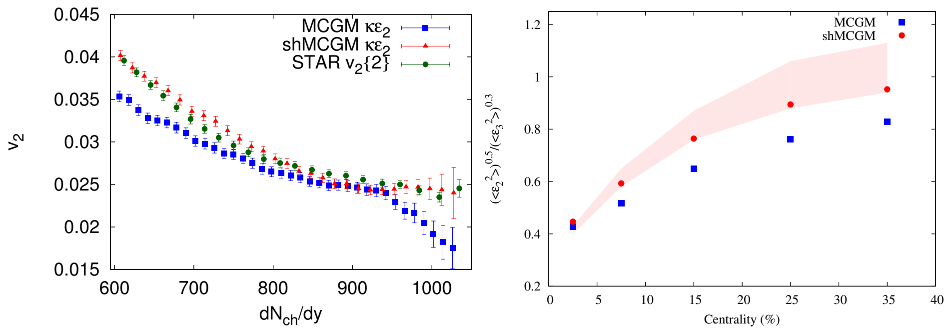

Fig. 1. (Left) The centrality dependence of v_2 for U+U at $\sqrt{s_{NN}} = 193$ GeV as obtained in MCGM and shMCGM. The experimental data is from Ref. [15]. (Right) The centrality dependence of the ratio of r.m.s. ε_2 to ε_3 compared between MCGM and shMCGM. Also shown is the band as proposed in Ref. [24] that is required to explain the correlation of v_2–v_3 in data assuming linear hydrodynamic response.

Another interesting point to note from Fig. 1 (left) is that ε_2 in the case of shMCGM is higher as compared to MCGM. In a typical mid-central collision where ε_2 is generated mainly because of the elliptical shape of the overlapped region, the ends of the major axis of the elliptical overlap region receive contribution from the boundary region of both nucleus. Hence, there is lesser energy deposition. The effect of shadow is weaker where lesser nucleons are expected to deposit energy. This leads to milder shadowing effect at the ends of the major axis, which effectively enhances the ellipticity in shMCGM compared to MCGM. Similar arguments also show that models based on gluon-saturation physics are expected to generate higher ε_2 as compared to MCGM [23].

The correlation between the even–odd harmonics largely stem from the ε_2–ε_3 correlation of the initial state (IS). Starting from the observed correlation in the data of v_2–v_3 at the LHC, an allowed band for the ratio of r.m.s. values of ε_2 to ε_3 was obtained in Ref. [24] within the realm of linear hydrodynamic response to the initial geometry. In Fig. 1 (right), we have shown this band. We also show the values obtained for the same quantity in MCGM and shMCGM. The enhancement of ε_2 in shMCGM as compared to MCGM also helps here — it pushes the prediction for the ratio of r.m.s. of ε_2 to ε_3 into the band that is favoured by data unlike the case of MCGM which underpredicts as compared to the band.

We now turn our attention from the mean geometric properties in the IC to their fluctuations. We first analyse the E/E distributions of the ε_n scaled by their ensemble average values and compare with that of IP-Glasma [9] as well as ATLAS data of v_n [17,18]. As long as the hydrodynamic response is linear ($v_n = k_n \epsilon_n$, where k_n is a constant), we expect the E/E distributions of $\varepsilon_n/\langle\epsilon_n\rangle$ to be a good representative of $v_n/\langle v_n\rangle$. In Fig. 2, we have plotted the E/E distribution plots for ε_2 for the following centrality classes: (0–5)%, (10–15)% and (20–25)%. Overall, there is good quantitative agreement between shMCGM and data as well as IP-Glasma. It is well-known that the standard MCGM produces a broader E/E distribution as compared to data as well as IP-Glasma results [12,25]. However, as already argued earlier in Ref. [20], the shadowing effect *shadows* the participants as well as their E/E fluctuations in a position which eventually results in narrower E/E distribution that is in good agreement with data and IP-Glasma predictions.

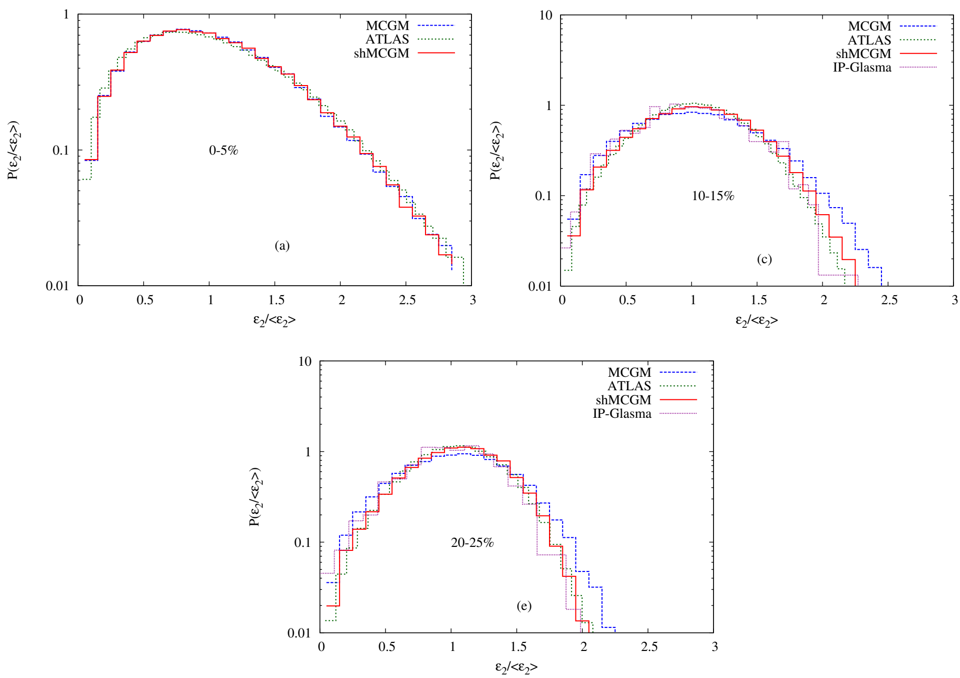

Fig. 2. (Colour on-line) The E/E distribution of ε_2 compared between data [17,18], IP-Glasma, MCGM and shMCGM.

Overall, the inclusion of nucleon shadowing in the IC of HICs has significant phenomenological consequences. Here, we have shown for observables pertaining to mid-rapidity like centrality dependence of v_2 in U+U and E/E distributions of elliptic flow in Pb+Pb is significantly affected by nucleon shadowing leading to better agreement between data and model.

REFERENCES

[1] A. Bialas, M. Bleszynski, W. Czyz, *Nucl. Phys. B* **111**, 461 (1976).
[2] K.J. Eskola, K. Kajantie, P.V. Ruuskanen, K. Tuominen, *Nucl. Phys. B* **570**, 379 (2000).
[3] D. Kharzeev, M. Nardi, *Phys. Lett. B* **507**, 121 (2001).
[4] D. Kharzeev, E. Levin, M. Nardi, *Phys. Rev. C* **71**, 054903 (2005).
[5] T. Hirano *et al.*, *Phys. Lett. B* **636**, 299 (2006).
[6] M.L. Miller, K. Reygers, S.J. Sanders, P. Steinberg, *Annu. Rev. Nucl. Part. Sci.* **57**, 205 (2007).
[7] W. Broniowski, M. Rybczynski, P. Bozek, *Comput. Phys. Commun.* **180**, 69 (2009).
[8] B. Schenke, P. Tribedy, R. Venugopalan, *Phys. Rev. Lett.* **108**, 252301 (2012).
[9] C. Gale *et al.*, *Phys. Rev. Lett.* **110**, 012302 (2013).
[10] M. Rybczynski, W. Broniowski, G. Stefanek, *Phys. Rev. C* **87**, 044908 (2013).
[11] A. Goldschmidt, Z. Qiu, C. Shen, U. Heinz, *Phys. Rev. C* **92**, 044903 (2015) [arXiv:1507.03910 [nucl-th]].
[12] H. Niemi, K.J. Eskola, R. Paatelainen, *Phys. Rev. C* **93**, 024907 (2016) [arXiv:1505.02677 [hep-ph]].
[13] R.D. Woods, D.S. Saxon, *Phys. Rev.* **95**, 577 (1954).
[14] H. Song *et al.*, *Phys. Rev. Lett.* **106**, 192301 (2011) [*Erratum ibid.* **109**, 139904 (2012)].
[15] L. Adamczyk *et al.* [STAR Coll.], *Phys. Rev. Lett.* **115**, 222301 (2015).
[16] J.S. Moreland, J.E. Bernhard, S.A. Bass, *Phys. Rev. C* **92**, 011901 (2015).
[17] A.R. Timmins [ALICE Coll.], *J. Phys.: Conf. Ser.* **446**, 012031 (2013).
[18] G. Aad *et al.* [ATLAS Coll.], *J. High Energy Phys.* **1311**, 183 (2013).
[19] R.J. Glauber, *Phys. Rev.* **100**, 242 (1955).
[20] S. Chatterjee *et al.*, *Phys. Lett. B* **758**, 269 (2016) [arXiv:1510.01311 [nucl-th]].
[21] S. Ghosh *et al.*, *Phys. Rev. C* **93**, 054904 (2016) [arXiv:1601.03971 [nucl-th]].
[22] P.F. Kolb, J. Sollfrank, U.W. Heinz, *Phys. Rev. C* **62**, 054909 (2000).
[23] H.J. Drescher, A. Dumitru, A. Hayashigaki, Y. Nara, *Phys. Rev. C* **74**, 044905 (2006).
[24] E. Retinskaya, M. Luzum, J.Y. Ollitrault, *Phys. Rev. C* **89**, 014902 (2014).
[25] B. Schenke, P. Tribedy, R. Venugopalan, *Phys. Rev. C* **89**, 064908 (2014).